

NONLINEAR DEFORMABLE BODIES WITH UNILATERAL CONTACT INCLUDING FRICTION

Fernando S. Buezas, fbuezas@gmail.com

Department of Physics, Universidad Nacional del Sur, 8000, Bahía Blanca, Argentina and CONICET, Argentina

Marta B. Rosales, mrosales@criba.edu.ar

Department of Engineering, Universidad Nacional del Sur, 8000 Bahía Blanca, Argentina and CONICET, Argentina

Carlos P. Filipich, cfilipich@gmail.com

CIMTA,FRBB, Universidad Tecnológica Nacional, 8000 Bahía Blanca, Argentina and Department of Engineering, Universidad Nacional del Sur, 8000 Bahía Blanca, Argentina

Abstract. *The study of the interaction between two deformable bodies that collide is of great interest since desired effects as a stable contact or undesired ones, as the failure of a mechanical part, can be predicted. In this work, a Signorini type contact model with impact considering large rotations and deformations is addressed. Both the static and dynamic Coulomb friction (dry friction) at the contact region are considered. The problem is stated using the Continuum Mechanics formulation in two and three dimensions with the Lagrangian description employing the two Piola-Kirchhoff stress tensors with linear or non-linear constitutive equations. The governing equations are solved through a general purpose software oriented to solve partial differential equations by using a finite element discretization. The impact of a deformable body on a rigid boundary or on other deformable body are tackled. Also a three-dimensional problem is addressed (e.g. a spheric ball impacting over a rigid surface). Numerical illustrations include parametric studies on the energy, the impulse forces and the time of contact for different initial conditions and materials. Finally a comparison among the models is showed.*

Keywords: *deformable bodies, unilateral contact, friction, lagrangian description*

1. INTRODUCTION

The classical theory of contact in Mechanics beginning with Hertz (Hertz, 1881) is restricted to frictionless surfaces and perfectly elastic solids undergoing small deformations. By the second half of past century, important progress were achieved to overcome these restrictions. A correct statement of the friction phenomenon has permitted the extension of the elastic theory to the sliding and friction of rolling elements. At the same time, the linear visco-elastic and plasticity theories have contributed to address deformations and stress when inelastic bodies are in contact. Reference books including modern approaches in this field are Gladwell (1980) and Johnson (1987). In more specific cases dealing with contact between very hard and soft bodies, such as glass and rubber surfaces, slipping noise phenomena are studied using stress waves (Barbarin, 1997). Monerie and Raous (2000) addressed the coupling of adhesion and unilateral contact among matrix/fiber interfaces with applications to composite materials. Diverse frictions regimes were addressed by Challen and Oxley (1979). Chabrand, Chertier, Dubois and Martinet (1998) modeled plasticity issues in sheet metal forming problems and developed various computational models as reported by Chabrand, Dubois and Raous (1998). Given the enormous advances in the computational sciences and in particular, in its application to the computational mechanics, a large number of related work has been published during the last decades (Chabrand, Dubois and Raous, 1998). A comprehensive review on articles dealing with mathematical, numerical and computational issues within Contact Mechanics may be found in Raous et al. (1995).

2. EQUATIONS OF MOTION

If the problem is stated in the *lagrangian* reference, only the following equation has to be solved (Gurtin, 1981; Wang and Truesdell, 1973),

$$\nabla_X \cdot \mathbf{P} + \rho_0 \mathbf{b} = \rho_0 \mathbf{A} \quad (1)$$

where \mathbf{P} is the first Piola-Kirchhoff stress tensor, $\rho_0 = \rho(\mathbf{X}, t_0)$ is the mass density of the initial configuration, $\mathbf{A} = \dot{\mathbf{V}} = \frac{\partial \mathbf{V}}{\partial t} = \frac{\partial^2 \mathbf{x}}{\partial t^2}$ is the acceleration field, \mathbf{b} are the body forces and, $\mathbf{x} = \mathbf{x}(\mathbf{X}, t)$ is the position vector. Notation ∇_X or $\nabla_X \cdot$ represent the gradient or the divergence with respect to the material coordinates X . Within this frame, the boundary conditions are imposed on the initial boundary which position is known by hypothesis. Thus, the problem at the boundary as well as the initial conditions and the equations of motion are fully stated. Once the differential problem is solved, both the position of the boundary as well as the location of any part of the body will be known for each instant.

The second Piola-Kirchhoff stress tensor may also be useful. It is symmetric and is given by $\mathbf{P} = \mathbf{F}\mathbf{S}$ where $[\mathbf{F}]_{ij} = \partial x_i / \partial X_j$ is the deformation gradient tensor, x_i is the *i*th component of the position vector (spatial description), X_j is the

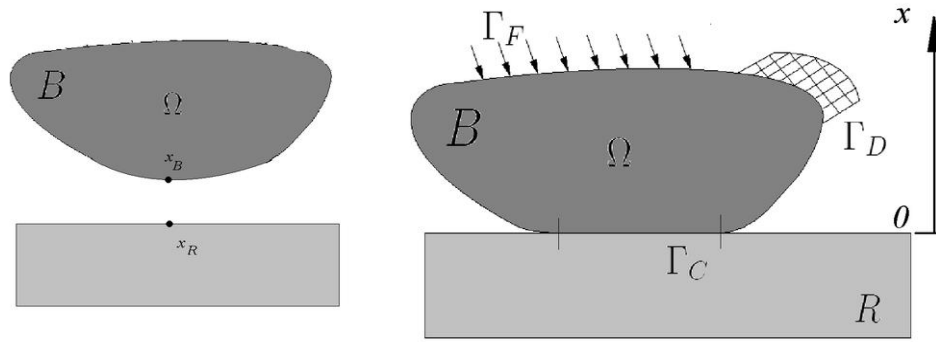


Figure 1. Scheme of the contact between a deformable body against a rigid contact.

j th component of the position vector (material description), \mathbf{X} . Then the equations of motion can be rewritten as follows,

$$\nabla_X \cdot (\mathbf{F}\mathbf{S}) + \rho_0 \mathbf{b} = \rho_0 \mathbf{A}. \quad (2)$$

The next relationship relates \mathbf{P} , \mathbf{S} and σ (the Cauchy stress tensor —spatial description)

$$\mathbf{F} \cdot \mathbf{S} = (\det \mathbf{F}) \sigma (\mathbf{F}^{-1})^T = \mathbf{P} \quad (3)$$

2.1 Constitutive equations

In this work, we will deal with elastic materials which satisfy

$$\mathbf{S} = g(\mathbf{E}) \quad (4)$$

where $[\mathbf{E}]_{ij} = \frac{1}{2} \left(\frac{\partial u_i}{\partial X_j} + \frac{\partial u_j}{\partial X_i} + \frac{\partial u_k}{\partial X_i} \frac{\partial u_k}{\partial X_j} \right)$ is the *lagrangian* finite strain tensor (or Green-St. Venant) and $\mathbf{u} = \mathbf{x}(\mathbf{X}, t) - \mathbf{X}$ is the displacement vector. In particular, the following constitutive law is proposed,

$$\mathbf{S} = \lambda \text{tr}(\mathbf{E})\mathbf{I} + 2\mu\mathbf{E} \quad (5)$$

where λ and μ are constants. This law is also known as St. Venant–Kirchhoff material model (Truesdell and Noll, 2004). A simple and interesting model of a hyperelastic material is given by the following relationship

$$\mathbf{S} = \mu (\mathbf{I} - \mathbf{C}^{-1}) + \lambda (\ln J) \mathbf{C}^{-1} \quad (6)$$

that describes a Neo-hookean compressible solid. λ and μ are constant, $\mathbf{C} = \mathbf{F}^T \cdot \mathbf{F}$ is the Green's deformation tensor and $J = \det(\mathbf{F})$. Moreover, if $J = 1$ in Eq. (6), a Neo-hookean incompressible solid is modeled.

2.2 Unilateral contact

As a first approach to the contact model, let us suppose that a deformable body interacts with a rigid and fixed obstacle. The contact condition is that the deformable body does not penetrate in the rigid obstacle.

2.2.1 Signorini problem

Let a body B occupy the domain Ω in a two- or three-dimensional space (Figure 1). The body boundary $\Gamma = \Gamma_F \cup \Gamma_D \cup \Gamma_C$ is smooth enough and it is in contact with a rigid fixed body. Part Γ_F of the boundary Γ corresponds to the boundary region at which the stresses are prescribed (natural conditions to the problem (1)). Γ_D is the region where the displacements are prescribed (geometric conditions) and Γ_C corresponds to the part in contact with the rigid body. At the contact region Γ_C , the displacements $\mathbf{v} = \mathbf{x}_B - \mathbf{x}_R$ are the difference between the coordinate of the point at the deformable body boundary and the corresponding one at the boundary rigid body (See Figure 1). Signorini problem (unilateral contact) is stated as follows

$$v_N \leq 0; \quad t_{cN} \leq 0; \quad u_N t_{cN} = 0 \quad (7)$$

1. No contact $\Rightarrow v_N \leq 0$ and $t_{cN} = 0$

2. Contact $\Rightarrow v_N = 0$ and $t_{cN} \leq 0$

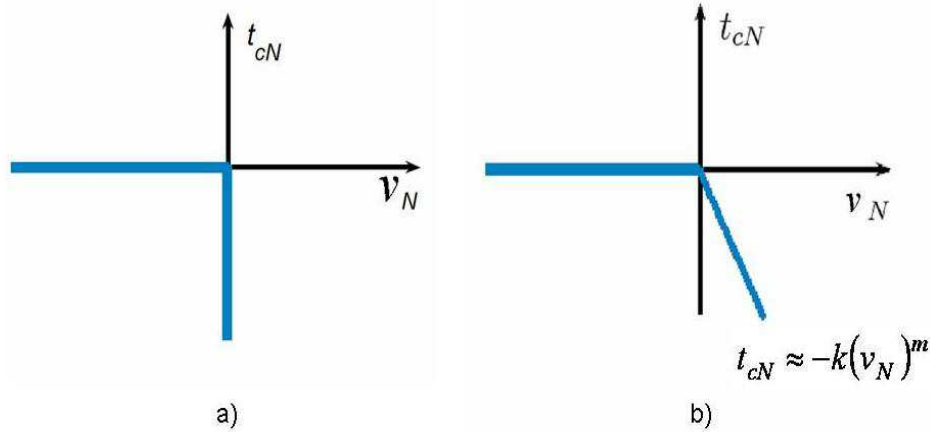


Figure 2. Signorini problem. a) multi-valued restriction; b) regularization.

Conditions (7) constitute a non-continuous or non-smooth problem since t_{cN} is a multi-valuated application of the v_N field (or simply t_{cN} is not a function of v_N). From the Analytical Mechanics viewpoint (Goldstein, 1980), Signorini conditions result in a non-holonomic ligatures problem due to the inequalities. This is reflected in the fact that neither the stresses nor the contact surface are known before solving the problem. If it were solved, the deformation could be calculated but they are necessary to the classical statement of the boundary. In other words, in Continuum Mechanics, the boundary conditions have to be known to solve the problems. However, Signorini problem gives the boundary conditions an unknown character. Figure 2a shows the multi-valuated feature of the restriction (7).

2.2.2 Extension to the contact between two deformable bodies.

When dealing with infinitesimal strains and displacements, the contact problem is easily solved by introducing a change of variable in the Signorini problem (7) which is now double

$$\text{BODY B1} \begin{cases} d(x_1, x_2) \leq 0 \\ t_{cN1} \leq 0 \\ x_1 t_{cN1} = 0 \end{cases} \quad \text{and} \quad \text{BODY B2} \begin{cases} d(x_2, x_1) \leq 0 \\ t_{cN2} \leq 0 \\ x_2 t_{cN2} = 0 \end{cases} \quad (8)$$

where $d(x_1, x_2)$ is the distance between \mathbf{x}_1 (B1) and \mathbf{x}_2 (B2). When infinitesimal displacements are assumed, then unit vectors satisfy $\mathbf{N}_2 = -\mathbf{N}_1$ and the pair of points \mathbf{x}_1 and \mathbf{x}_2 are known before the problem is solved, and are located on the normal to each surface. Instead, if the displacements or strains are considered finite, there is no knowledge about which pair of points will contact, neither the corresponding normal unit vectors. In this case, the minimum of the distances between all possible pair of points has to be evaluated as well as the unit normal vectors.

$$\begin{cases} \min(d(x_1, x_2)) \leq 0 \\ t_{cN1} \leq 0 \\ x_1 t_{cN1} = 0 \end{cases} \quad \begin{cases} \min(d(x_2, x_1)) \leq 0 \\ t_{cN2} \leq 0 \\ x_2 t_{cN2} = 0 \end{cases} \quad (9)$$

2.2.3 Regularization of the non-holonomic Signorini problem

The contact law (7) stated before is non-holonomic, since no regular restriction given by an equality exists. Instead, the problem contains a restriction given by a set of inequalities. Furthermore, when contact appears, neither the stress value nor the displacement is defined. This alternation between natural and geometric conditions gives the problem the non regular character since the moment in which each one stands, is an unknown. The regularization of the contact problem consists in the replacement of the rigid condition (7) by a smooth or regular one. The non holonomic problem is replaced by a problem without ligatures. The boundary condition will be always natural, by imposing a functional relationship between stresses and displacements.

$$t_{cN} = \begin{cases} -k(v_N)^m & \text{if } v_N > 0 \\ 0 & \text{if } v_N \leq 0 \end{cases} \quad (10)$$

where k is a sufficiently large number in order for (10) to approximate (7) and m an arbitrary constant ($m = 1$ for the linear approximation).

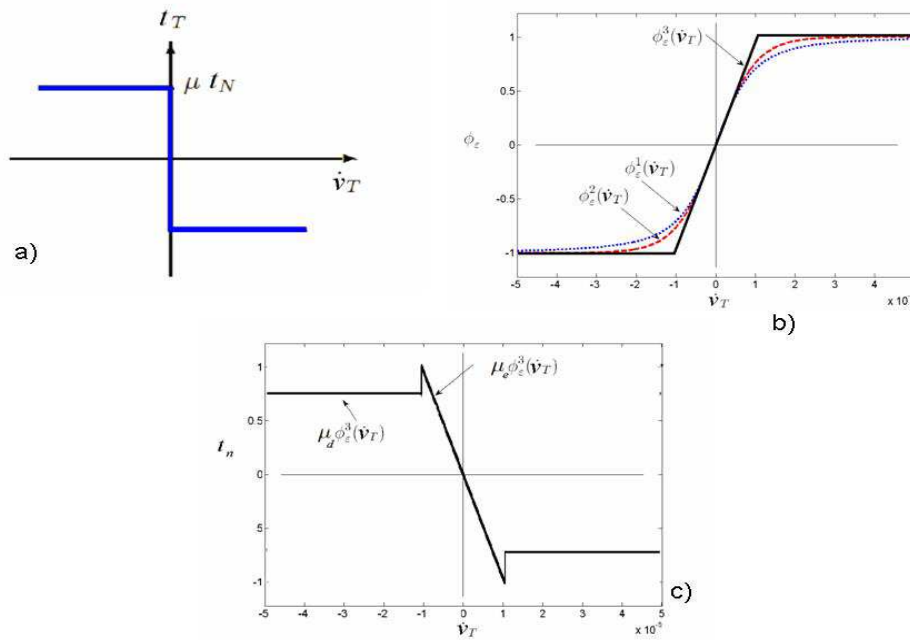


Figure 3. a) Coulomb friction law; b) Regularization of the friction law with $\epsilon = 10^{-1}$; c) Coulomb law regularized with an approximating function Φ_ϵ^3 and including static and dynamic friction.

2.3 Friction

2.3.1 Coulomb friction

This well-known model was introduced by Amontons in 1699 (Amontons and Sasada, 1999) and later developed by Coulomb in 1785 (Coulomb, 2002). However the global character of the model when dealing with rigid bodies yielded a very rough approximation. But when applied to deformable bodies, a more realistic result is obtained. Even the “stick and slip” phenomenon (alternation of static and dynamic friction). The friction force of a body against the other is always less or equal to a factor times the force normal to the contact surface. It is colinear to the contact surface and its sense is contrary to the velocity with which the two bodies slide, and is describes as follows

$$t_T \leq \mu t_N \begin{cases} \text{if } t_T < \mu t_N \rightarrow \dot{v}_T = 0 \\ \text{if } t_T = \mu t_N \rightarrow \dot{v}_T = -\lambda t_T \end{cases} \quad (11)$$

where μ is the friction coefficient, λ is a real number and \dot{v}_T is the velocity tangent component (See Figure 3a). As can be observed, the friction law must be expressed not only in terms of the normal force but also as function of the velocity since it depends on the previous evolution. The static friction is included in (11).

2.3.2 Regularization of the Coulomb model

The friction law described above is non-regular since no univocal functional relationship exists to relate $t_T = t_T(\dot{v}_t)$ for all values of the velocity. For instance, when the velocity is null, the friction force is not defined. For this situation, the functional relationship is with other kinematic quantities. In fact, it will be equal and opposite to the force that tends to slide one body against the other. But, again, this law can be regularized (Raous, 1999), approximating with a function $\phi(\dot{v}_T)$ similar to a step function, in such a way that the friction law may be written as

$$t_T = -\mu \phi_\epsilon(\dot{v}_T) |t_N| \quad (12)$$

where ϵ is a parameter that when tending to zero, $\phi_\epsilon(\dot{v}_T) \rightarrow \text{step}(\dot{v}_T)$. Examples of this type of functions are: $\phi_\epsilon^1(\dot{v}_T) = \frac{\dot{v}_T}{\sqrt{\dot{v}_T^2 + \epsilon^2}}$, $\phi_\epsilon^2(\dot{v}_T) = \tanh \frac{\dot{v}_T}{\epsilon}$. The three alternatives are shown in Figure 3b. In the present study, the following function is adopted

$$\phi_\epsilon^3(\dot{v}_T) = \begin{cases} -1 & \text{if } \dot{v}_T < -\epsilon \\ \frac{\dot{v}_T}{2\epsilon} & \text{if } -\epsilon < \dot{v}_T < \epsilon \\ 1 & \text{if } \dot{v}_T > \epsilon \end{cases} \quad (13)$$

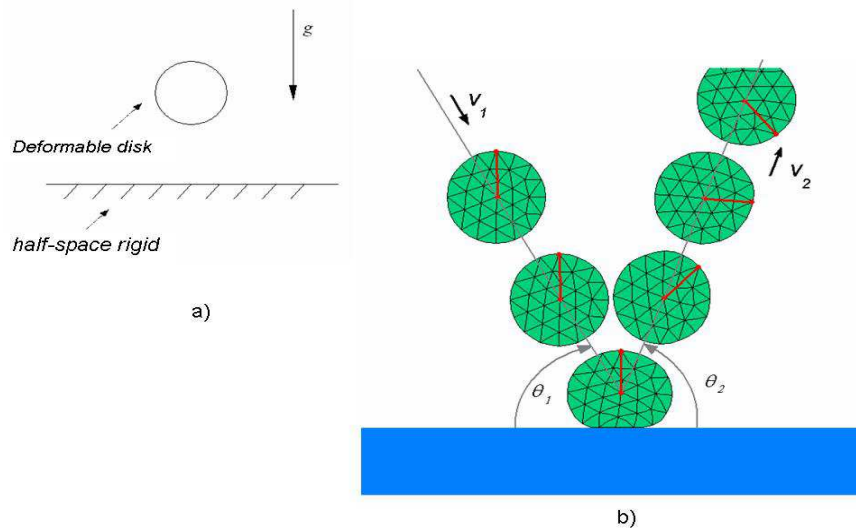


Figure 4. Plane disc impacting and rolling on a rigid surface. a) Geometry of the problem; b) Collision of the deformable disc against the rigid surface for various time instants.

From the numerical viewpoint, it will be appropriate to take a ε sufficiently small. It is easy to observe that $\lim_{\varepsilon \rightarrow 0} \phi_{\varepsilon}^{1,2,3}(\dot{v}_T) = \text{step}(\dot{v}_T)$. As is usually accepted, the contact friction exhibits two slightly different behaviors for static or dynamic friction. In order to include the static friction in the model, a modification is introduced in (13). The static friction is supposed to be valid in $-\varepsilon < \dot{v}_T < \varepsilon$ and dynamic elsewhere. In Eq.(12), coefficient $\mu = \mu_e$ or μ_d where μ_e corresponds to the static modulus and μ_d to the dynamic one, usually smaller than the first coefficient. Figure 3c shows the modified law as is adopted in the present study.

3. NUMERICAL ILLUSTRATIONS

The resulting differential problem was solved using finite element discretization. This task was performed with the help of FlexPDE software (PDE Solutions Inc, 2009) which is a scripted finite element model builder and a numerical solver.

3.1 Plane disc impacting and rolling on a rigid surface

The behavior of a plane disc impacting against a rigid surface is studied in order to calibrate the computational model of the contact between a deformable and a rigid body. Dry (Coulomb) friction is considered. The problem of the disc falling and impacting against the rigid body is simulated with the theoretical formulation above presented and solved using the commercial package FlexPDE. The disc is of radius $r = 0.05m$, the mass density is $\rho = 1722kg/m^3$ and the material is governed by the constitutive law (5) choosing values of λ and μ in such a way that, when dealing with small strains, they are in the elastomeric material (rubber) range. Recall that $\lambda = \nu E / (1 + \nu)(1 - 2\nu)$, $\mu = E / 2(1 + \nu)$ where E is the elastic modulus and ν is the Poisson coefficient. In the present illustration, $E = 7 \cdot 10^6 Nm^{-2}$ and $\nu \rightarrow 0.5$. The equation of motion (2) is stated along with the boundary conditions given by the Eqs. (7) and (11) with the regularizations (10) and (12), respectively. Figure 4a contains an scheme of the problem geometry. Different initial conditions lead to different dynamics.

The simpler situation to start the study is the disc falling vertically. Figure 4b depicts the body trajectory at various time instants including the impact on the rigid surface, after being dropped with an oblique incidence (initial angle θ_1 and an initial velocity v_1). Studies of this type in more elementary models may be found in Jafri (2004). The value of the angle of incidence was taken $\theta_1 = \pi/3$ and $v_1 = 12 m/s$. A Coulomb type friction (12) was considered with a dynamic coefficient $\mu_d = 0.5$ and a static one $\mu_e = 0.7$. Since the dynamic is computationally simulated, any derived parameter can be evaluated. For instance, the total contact force can be found integrating the product of the accelerations and the density of all the body domain, i.e. $\mathbf{F}(t) = \int_{V_{ol}} \mathbf{A}(\mathbf{X}, t) \rho_0 dV$. The vertical component of this force, is plotted in Figure 5a. The oscillations are due to the multiple reflexions of the impact waves on the disc boundary. The friction force is shown in Figure 5b and the zoom corresponds to the instability born from the alternation between the static and dynamic behaviors. This instability is characterized by a discontinuity in the acceleration due to the sudden change in the type of friction.

The disc energy variation is shown in Figure 6a. The total energy remains constant until contact starts. At this moment,

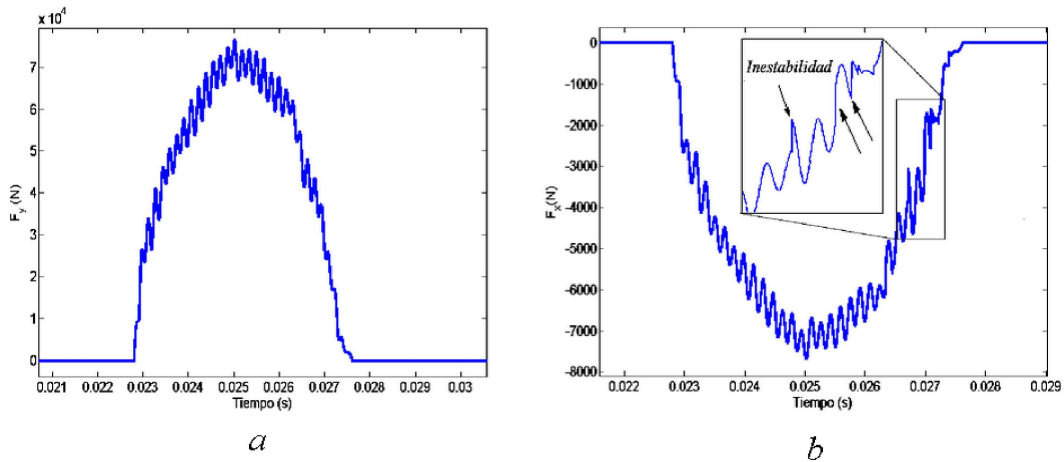


Figure 5. Contact force. a) Normal force; b) Friction force.

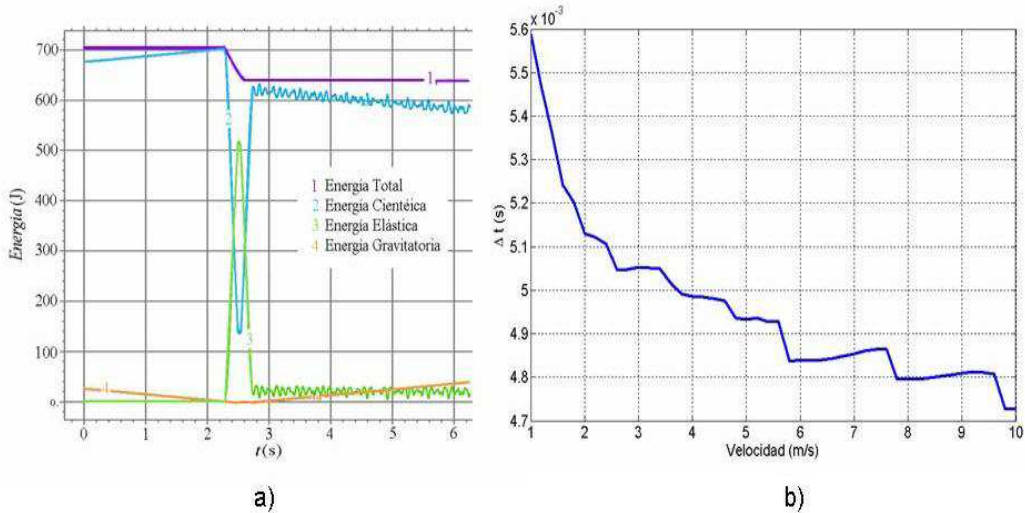


Figure 6. a) Energy of the disc during the contact as function of time; b) time of contact as a function of the initial velocity.

it decreases and then, before the contact finishes, is again constant. This is due to the fact that, in the first instants, the friction is dynamic and then, approximately during the last third of the time of contact, becomes static (conservative). In this last third, the disc rolls without sliding. It is also noticeable how the elastic energy is null before the contact and during it, fluctuates together with the kinetic energy. Other interesting issue in this study, is the determination of the time the bodies remain in contact which can be estimated by observing when the force is not null. In the present example ($v_1 = 12 \text{ m/s}$), for instance, this time was calculated to be $\Delta t = 0.0045 \text{ s}$. Figure 6b shows a graph of the time of contact vs. initial velocity. For this case, the disc impacts normally to the surface, i.e. $\theta_1 = \pi/2$ and no friction nor gravity are considered. It may be observed that, in general, the time of contact decreases with the velocity of incidence. However, the decrement is not monotonic and it looks stepped with small increases between steps, which is an unexpected result. This behavior may be explained by the fact that when the velocity increases, the waves are reflected on the disc boundary fewer times (the steps are related to the number of internal wave reflections). The angles of incidence and reflection are different as may be observed in Figure 4b. A model that represents an elastomeric-type model more realistically, is given by Eq. (6). This nonlinear constitutive model demands larger computational times. However, when dealing with a smooth impact, Figure 7a, no noticeable differences arise. On the contrary, when large deformations are involved, Figure 7b, the time of contact is larger. The examples shown in Figure 7 correspond to a normal incidence and it may be observed that the contact time is larger for the material governed by (5). The contact time vs. initial velocity of a body modeled with a Neo-hookean constitutive law (6) is depicted in Figure 8. As before, the disc is normally impacting the surface ($\theta_1 = \pi/2$) and no friction nor gravity are considered. A monotonic decrease of the contact time as the velocity increase is observed which is different from the previous case (Figure 6b).

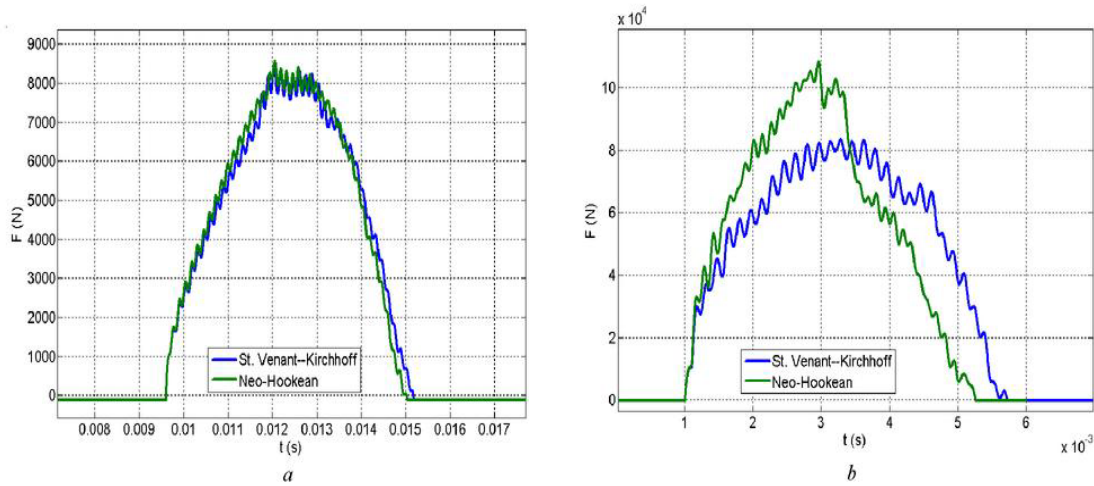


Figure 7. Contact force during the impact of the disc using St. Venant-Kirchhoff and Neo-hookean constitutive models.
 a) Velocity of incidence $v_1 = 1$ m/s; b) Velocity of incidence $v_1 = 10$ m/s.

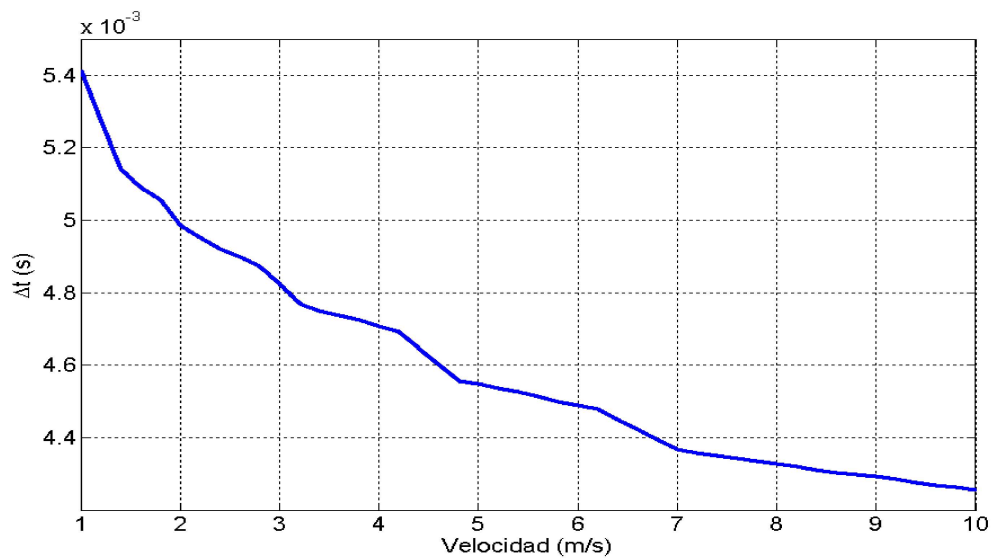


Figure 8. Contact time for a body governed by constitutive law (6).

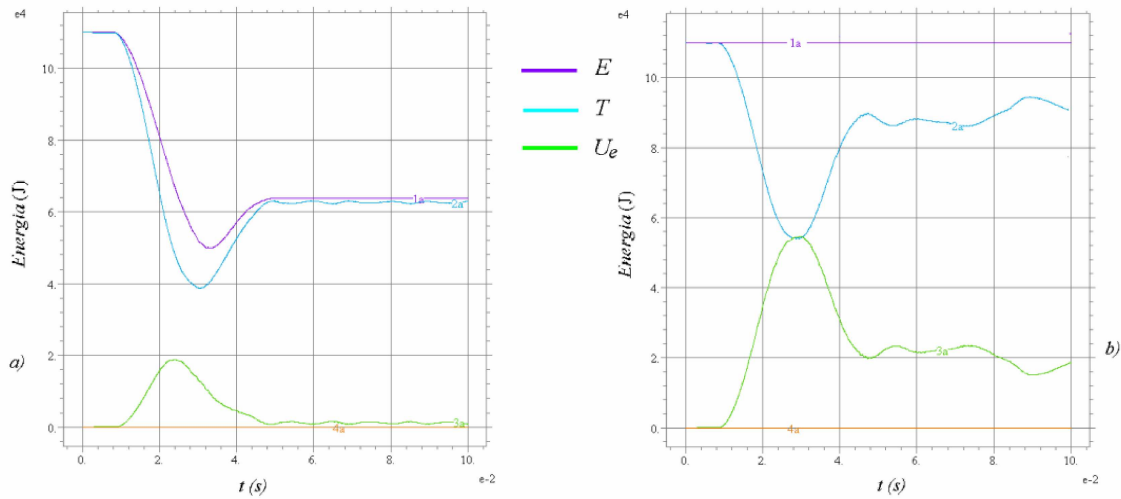


Figure 9. Energy variation in the impact of two deformable bodies. a) Only disc; b) disc and rectangular body.

3.2 Disc impacting against a deformable body

Dealing with the impact of a deformable body against other adds complexity to the problem since the positions of points of each boundary that will contact are unknown. Here, Eq.(9) should be employed at the cost of increasing the CPU time. Not only the body boundary trajectories has to be monitored but also the minimum distance at each instant of time. A strategy to avoid the calculus of the minimum distances, as forced by conditions (9), is to construct a new regularizing function such that

$$a(c_1) = \begin{cases} -k(d(x_1, x_2)) & \text{if } d < \varepsilon \\ 0 & \text{if } d > \varepsilon \end{cases} \quad a(c_2) = \begin{cases} -k(d(x_2, x_1)) & \text{if } d < \varepsilon \\ 0 & \text{if } d > \varepsilon \end{cases} \quad (14)$$

where c_1 and c_2 are the boundaries of the bodies 1 and 2, $d(x_1, x_2)$ is the distance between point x_1 (body c_1) and point x_2 (body c_2) and ε is a sufficiently small number. Then the normal component of the Piola- Kirchhoff stress at the c_1 arising due to its interaction with the body 2 is denoted t_{cN_1} and analogously, t_{cN_2} . They are written as

$$t_{cN_1} = \sum_{\forall x \in c_1} a(c_2) \quad t_{cN_2} = \sum_{\forall x \in c_2} a(c_1) \quad (15)$$

If ε is approximately in the separation order of the points at each boundary and if number k is sufficiently large, then it could be assured that each point of body 1 will interact with a single point of body 2, since a single $a(c_1) \neq 0$ and a $a(c_2) \neq 0$ will exist for each of the boundaries. The sum will be reduced to these unique values and it will not be necessary to search the point that minimizes the distance and consequently, the one that is in contact. The disc of radius $r = 0.5 \text{ m}$ impacts on a body with dimensions $10 \text{ m} \times 2 \text{ m}$ both with identical elastic characteristics. The second body is not externally restricted. Neither friction nor gravitational forces were considered and the governing constitutive law (5) was stated with $E = 7 \cdot 10^6 \text{ Nm}^{-2}$, $\nu \rightarrow 0.5$ and $\rho = 1722 \text{ kg/m}^3$. The initial conditions of the disc are velocity of incidence $v = 10 \text{ m/s}$ with normal direction to the rectangular plane which is at rest. After the collision, the disc is reflected and the rectangular body is directed downwards. Finally, the variations of the energy are displayed in Figure 9. The variation for the disc energy is shown in Figure 9a and the total energy, in Figure 9b. Since the system is conservative, the total energy remains constant. This feature is used to test the numerical convergence of the solutions.

3.3 Spherical body impacting on a rigid surface

The illustrations above presented described 2D finite elements models. However no limitation, besides the computational requirements, exist to extend the approach to three-dimensional bodies. The contact is modeled in an identical way. The ball material is modeled with constitutive equation (5) and, as before, $E = 7 \cdot 10^6 \text{ Nm}^{-2}$, $\nu \rightarrow 0.5$, $\rho = 1722 \text{ kg/m}^3$ and radius $r = 0.05 \text{ m}$. The initial condition is $v = 8 \text{ m/s}$ normal to the rigid body. The time of contact is, in this case, $\Delta t = 0.00603 \text{ s}$. For the disc case (2D model simulation), it was found $\Delta t = 0.0048 \text{ s}$. As before, the controls on the adaptive time step are tested by checking the energy which is constant since we are dealing with a conservative impact, Figure 10. The plot at the right depicts the variation of the impact force with time. The acceleration of the center of mass can be calculated as $\mathbf{A}_{CM} = (1/V) \int \int \int \mathbf{A}(\mathbf{X}, t) dV$ where V is the non-deformed volume of the body. The plots of

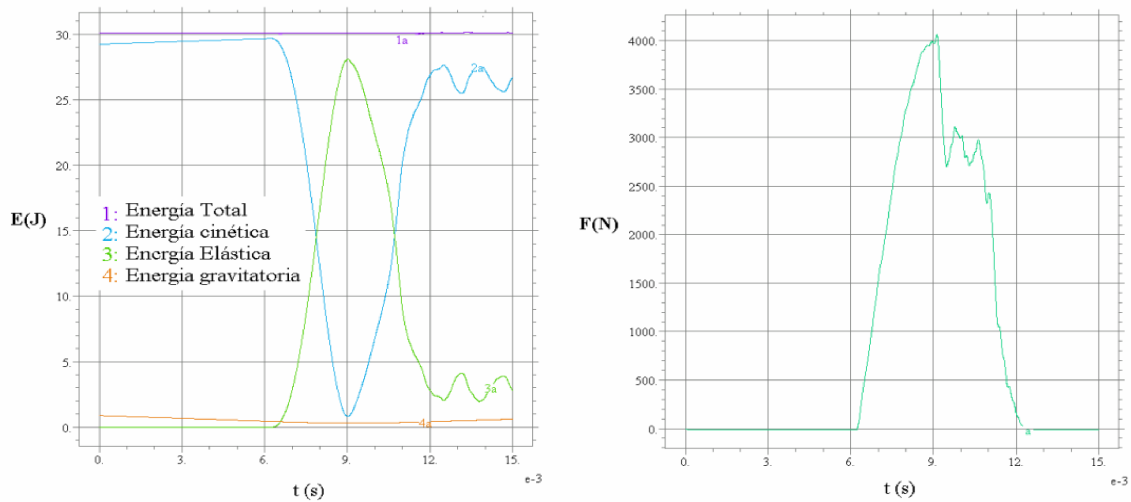


Figure 10. Spherical ball impacting on a rigid boundary. Energy and impact force as functions of time.

the acceleration in function of time for the 2D disc with the constitutive laws (5) and (6) and the ball with constitutive law (5) when they are impacted on a rigid semi-space, are shown in Figure 11. The contact time is always larger in the spherical ball case when the constitutive laws are, at least, similar.

4. CONCLUSIONS

The impact of bodies with contact and friction has been addressed within the Continuum Mechanics using the *lagrangian* reference. Some issues, as the regularization of both the contact and friction problems, were tackled. The proposed formulation was applied to three problems: a deformable plane disc impacting on a rigid plane, a deformable disc on a deformable plane body and finally, a deformable spherical ball impacting on a rigid solid. In all cases, the resulting differential problem was solved by means of a finite element discretization. Several conclusions can be drawn from the study above described. With respect to the physical-mathematical model, the mechanics of the unilateral contact was stated with arbitrary displacements and rotations in the *lagrangian* reference. It was shown that stick-slip (intermittent friction), vibro-impact, smooth slip phenomena can be appropriately reproduced. Parametric studies were carried out in impact and friction problems between two deformable bodies, studying the influence of the time of contact and the impulsive forces. Also comparison of different constitutive laws was accomplished. The energy studies permit the monitoring of the solution quality when dealing with conservative problems and understand the dissipation when friction leads to non-conservation patterns. An interesting result was found in the deformable disc-rigid plane impact case. The time of contact decreases with the increase of the velocity of incidence in a stepped fashion. A possible explanation is the fact that, in the impact, the elastic waves are reflected in an integer number of times within the disc limits; then, as the time of contact decreases, the waves reflect one time less, producing the step. As expected, the elastic models St. Venant-Kirchhoff and Neo-Hookean are similar when the velocities are low and the deformations small. As the velocities of incidence are higher, the Neo-Hookean yields a stiffer behavior.

5. ACKNOWLEDGMENTS

The authors are grateful to the financial support of SGCyT-Universidad Nacional del Sur, ANCyT and CONICET, all institutions from Argentina.

6. REFERENCES

- Amontons, G. and Sasada, T.: 1999, De la resistance cause'e dans les machines (1), *Journal of Japanese Society of Tribologists* **44**, 229–235.
- Barbarin, S.: 1997, *Instabilité et Frottement en Elasticité, Application à un Problème d'Ondes de Contrainte*, PhD thesis, Université de Provence, Marseille, France.
- Chabrand, P., Chertier, O., Dubois, F. and Martinet, F.: 1998, Variable friction coefficient model in sheet metal forming, *NUMIFORM98*, pp. 845–850.

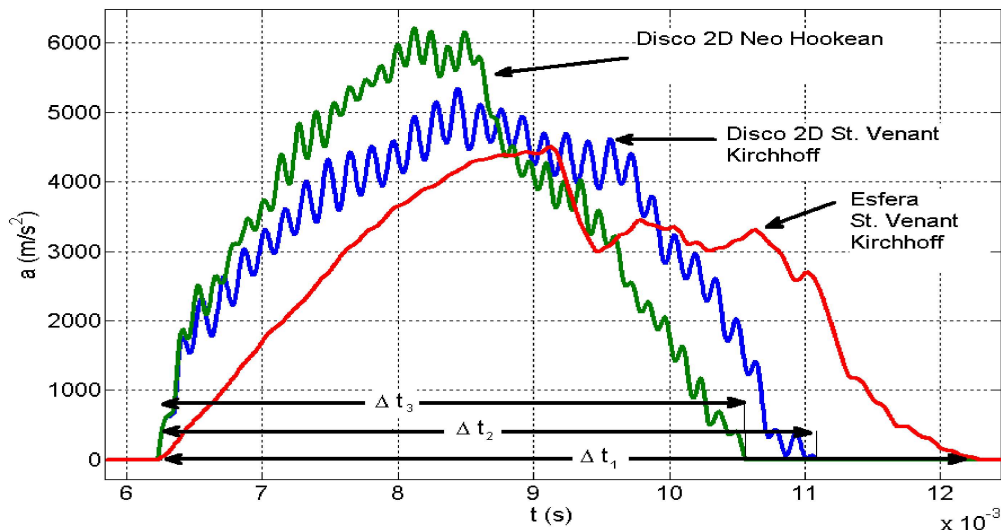


Figure 11. Comparison of accelerations of the center of masses of the disc with two constitutive models and the ball.

- Chabrand, P., Dubois, F. and Raous, M.: 1998, Various numerical methods for solving unilateral contact problems with friction, *Mathematical and computer modelling* **28**, 97–108.
- Challen, J. and Oxley, P.: 1979, An explanation of the different regimes of friction and wear using asperity deformation models, *Wear* **53**, 229–243.
- Coulomb, C.: 2002, *Théorie des machines simples*, Librairie scientifique et technique, Albert Blanchard, Paris.
- Gladwell, G.: 1980, *Contact Problems in the Classical Theory of Elasticity*, Kluwer Academic Publishers.
- Goldstein, H.: 1980, *Classical Mechanics*, 2nd. edition edn, Springer.
- Gurtin, M.: 1981, *An Introduction to Continuum Mechanics*, Academic Press.
- Hertz, H.: 1881, On the contact of elastic solids, *Journal Reine Angew Math* **92**, 156–171.
- Jafri, S.: 2004, *Modeling of impact dynamics of a tennis ball with a flat surface*, Master's thesis, Texas A&M University, USA.
- Johnson, K.: 1987, *Contact Problems in the Classical Theory of Elasticity*, Cambridge University Press.
- Monerie, Y. and Raous, M.: 2000, A model coupling adhesion to friction for the interaction between a crack and a fibre/matrix interface, *Zeitschrift für angewandte Mathematik und Mechanik* **80**, 205–208.
- PDE Solutions Inc., : 2009, *FlexPDE 6.0*.
- Raous, M.: 1999, *Quasistatic Signorini problem with Coulomb friction and coupling to adhesion*, New Developments in contact problems, Springer, chapter 3.
- Raous, M., Jean, M. and Moreau, J.: 1995, *Contact Mechanics*, Plenum Press.
- Truesdell, C. and Noll, W.: 2004, *The Non-Linear Field Theories of Mechanics*, Springer.
- Wang, C. and Truesdell, C.: 1973, *Introduction to Rational Elasticity*, Kluwer Academic Publishers.

7. Responsibility notice

The authors are the only responsible for the printed material included in this paper.